URBAN COMPLEXITY ESTIMATION INDICES BASED ON 3D DISCRETE WAVELET TRANSFORM OF REMOTELY SENSED IMAGERY : THE PRELIMINARY INTERPRETATION WITH LAND COVER MAP

Hee-Young Yoo [1], Kiwon Lee [2] and Byung-Doo Kwon [1]

[1] Dept. of Earth science Education, Seoul National University
[2] Div. of Information Engineering, Hansung University

E-mail: skyblue@mantle.snu.ac.kr, kilee@hansung.ac.kr and bdkwon@mantle.snu.ac.kr

ABSTRACT : Each class in remotely sensed imagery has different spectral and spatial characteristics. Natural features have relatively smaller spatial changes than spectral changes. Meanwhile, urban area in which buildings, roads, and cars are included is inclined to face more changes of spatial variation than spectral one. This study aims to propose the new urban complexity index (UCI) based on the 3D DWT computation of remotely sensed imageries considering these characteristics. And then we analyze relation between index and land cover map. The 3DWUCI values are related to class and the indices of urban area are greater than natural area. The proposed UCI could be used to express effectively the standard of urban complexity over a wide area.

KEY WORDS: 3D DWT, energy parameter, land-cover map, UCI

1. INTRODUCTION

Urban areas are growing more and more and the urban growth affects social environment such as prices, transportation and the quality of life as well as natural environment such as climate, water and ecology system. So, grasping an urbanization level is basic to analyze the relationship between urban and others. The majority of previous studies focused the quality of life in urban and utilized mainly GIS based statistical technique with population, building size, housing density, and road distribution data (Liu, 1976; Bederman & Hartshorn, 1984). However, collecting statistical data can be very time and cost-consuming.

In recent years, the use of remotely sensed data for urban studies has been increasing because remote sensing is useful to get information in broad area saving time and money. Forster (1983) developed a residential quality index in Sydney, Australia using LANDSAT MSS image. Remotely sensed data with conventional census data were used for the urban life quality index (Webar & Hirsch, 1992; Lo & Faber, 1997; Jun, 2006) However, these studies did not define new index using pixel values of remotely sensed imagery but use normalized difference vegetation index (NDVI), morphological technique and classification results.

This study aims to propose the new urban complexity index based on the 3D DWT computation of remotely sensed imageries. The 3D DWT is a scheme for analyzing volumetric data. In space-borne imageries, natural features such as water, forest and bare soil natural show small variation in spatial information. Meanwhile, urban area which consists in various buildings, houses, roads, and transportation facilities has more changes of spatial variation than spectral variation. The 3D DWT can be used to divide complex urban area and rural area with the consideration to these spectral and spatial properties because the 3D DWT is capable of computing both spectral and spatial variation.

2. 3D DISCRETE WAVELET TRANSFORM

2.1 Fundamentals

The 3D DWT expands the 1D wavelet theory into three dimensions. The 3D DWT decomposes data not only in row and column direction but also in depth direction. In terms of wavelet space decomposition, the 3D DWT can be constructed by a tensor product by

$$
\begin{aligned}
V^3 &= (L^x \oplus H^x) \otimes (L^y \oplus H^y) \otimes (L^z \oplus H^z) \\
&= L^x \otimes L^y \otimes L^z \oplus L^x \otimes L^y \otimes H^z \\
&\oplus L^x \otimes H^y \otimes L^z \oplus H^x \otimes L^y \otimes L^x \\
&\oplus L^x \otimes H^y \otimes H^z \oplus H^x \otimes L^y \otimes H^z \\
&\oplus H^x \otimes H^y \otimes L^z \oplus H^x \otimes H^y \otimes H^z
\end{aligned} \tag{1}
$$

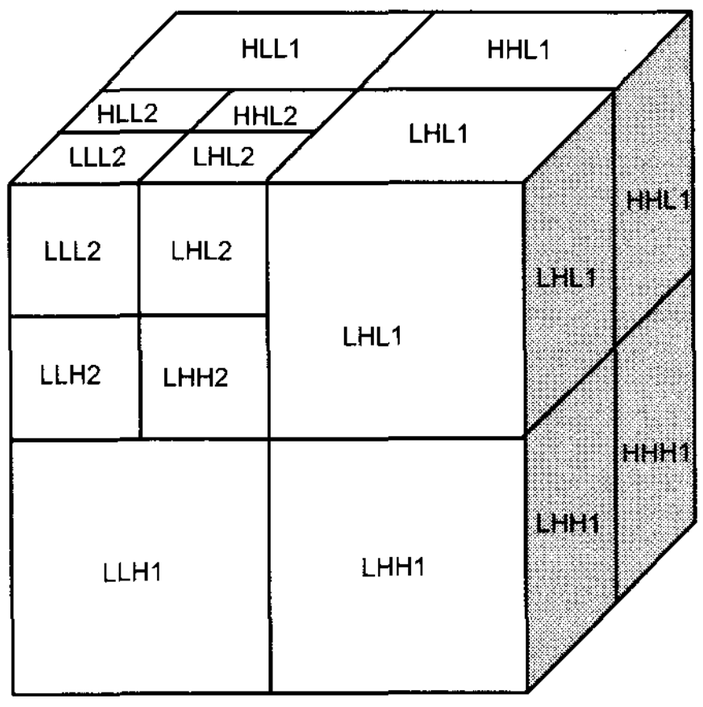

Figure 1. The Sub-band partition of 3D discrete wavelet transformation (two-level decomposition).

where $\oplus$ denotes space direct sum, H^{λ} and L^{λ} ; respectively, represent the high and low-pass directional filters along directions of λ-axis, where λ ={x, y, z} (Chen and Ning, 2004). After the 3D DWT is applied in one level, 8 sub-bands are created. Each sub-band is named by directions and frequency filter passed in: LLL, LLH, LHL, HLL, LHH, HLH, HHL, and HHH. (Yoo *et al*, 2007). The 3D DWT is substantially regarded as useful one on analyzing both spatial and spectral information. Figure 1 shows sub-band partition of 3D wavelet transformation in two level.

2.2 The energy parameter

The energy parameter of signal is the sum of the squares of wavelet coefficients and it is computed by sub-bands after wavelet decomposition process. The energy parameter is calculated by the equation 2. Equation 3 is for the energy parameter of 3D discrete wavelet transform.

$$E_m = \sum_{n=0}^{2^{M-m}-1} (T_{m,n})^2 \tag{2}$$

$$\varepsilon_f = \sum_{i=1}^{l} \sum_{j=1}^{m} \sum_{k=1}^{n} f_{i,j,k}^{2} \tag{3}$$

The energy parameter is calculated by sub-bands after wavelet decomposition and the energy parameter of each sub-band can be a favourable feature of texture because it indicates dominant spatial and spectral frequency channels of the original image (Fukuda & Hirosawa, 1999). The energy parameter is concentrated in LLL band. As the number passing a high-pass filter is increasing, the computed value of energy parameter decreases.

3. URBAN COMPLEXITY INDEX

Natural features which have relatively smaller spatial changes give much weight the energy of H components in band direction (LLH, LHH and HLH). Meanwhile, urban features are more changeable in row and column directions. In this case, the energy of L components in band direction (HHL, HLL and LHL) is higher value than the energy of H components. Putting these characteristics together, 3DWUCI is defined through the ratio of L components and H components in band direction. The index is defined as the sum of all H components by the sum of all L components in band direction (equation 4).

$$3DWUCI = \frac{E_{HLL} + E_{LHL} + E_{HHL}}{E_{LLH} + E_{LHH} + E_{HLH}} \tag{4}$$

Even though the overall brightness of imagery is different from each other, if the difference of value is same, the energy of all the rest band except that of LLL band is same altogether. Therefore the suggested indices have consistency regardless of overall brightness because the energy parameter of LLL band is not used. Figure 2 shows the flowchart for 3DWUCI calculation.

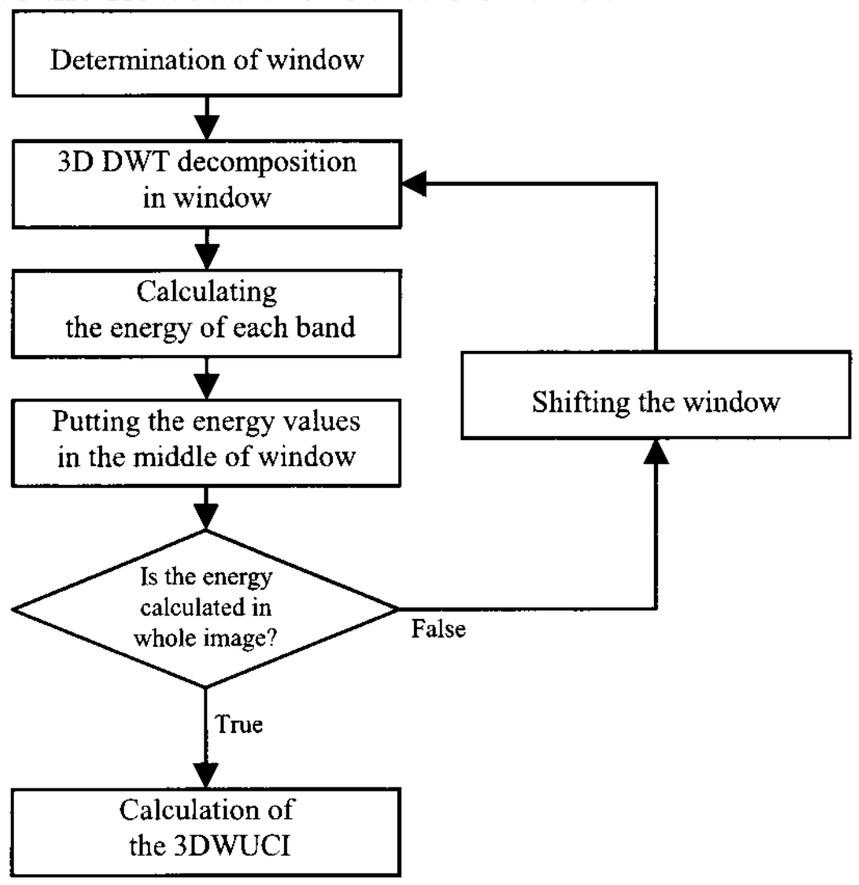

Figure 2. The flowchart of the 3DWUCI calculation procedure.

Firstly, the size of window is determined. The 3DWUCI is heavily influenced by window size even though the applied image which has the same resolution is used. The proposed method makes it possible that indices computation on window size what one wants to analyze or interpret. The used window size in this study is 8. Next, sub-image in window is decomposed through the 3D DWT. After a local window in an image is decomposed, the energy of each sub image is calculated. And then, we calculate the 3DWUCI using the energy values of 8 sub-bands from the 3D DWT. For the 3D DWT, the used basis function is the haar wavelet which is advantageous in the urban images containing buildings and road boundaries where pixel value changes dramatically and multi-spectral image has not have many bands. If any index is used, the greater index value means that city is more complex regardless of index.

4. APPLICATION AND DISCUSSION

Two images are used for this study and those images obtained from the urban area. One is Landsat7 ETM+ image (Figure 3 (a)). Landsat7 ETM+ imagery is covered with Seoul, Korea and has 8 bands with 15m (panchromatic band) and 30m (multi-spectral bands except thermal infrared band (band 6)) and 60m (thermal infrared band) spatial resolution, but 7 bands except panchromatic band are used. Another applied image is Ikonos image (Figure 3 (b)). Ikonos imagery on Hobart, Australia is one of ISPRS dataset collection (http://www.isprs.org/data/index.html) and is composed of red, green, blue, and near infrared bands (4m).

The 3DWUCIs are computed using two satellite images according to the procedure in figure 2. Figure 4(a) and

6(a) are the results of 3DWUCI computation with the same scale indicator. Figure 4(b) and 6(b) are land cover maps in each test area.

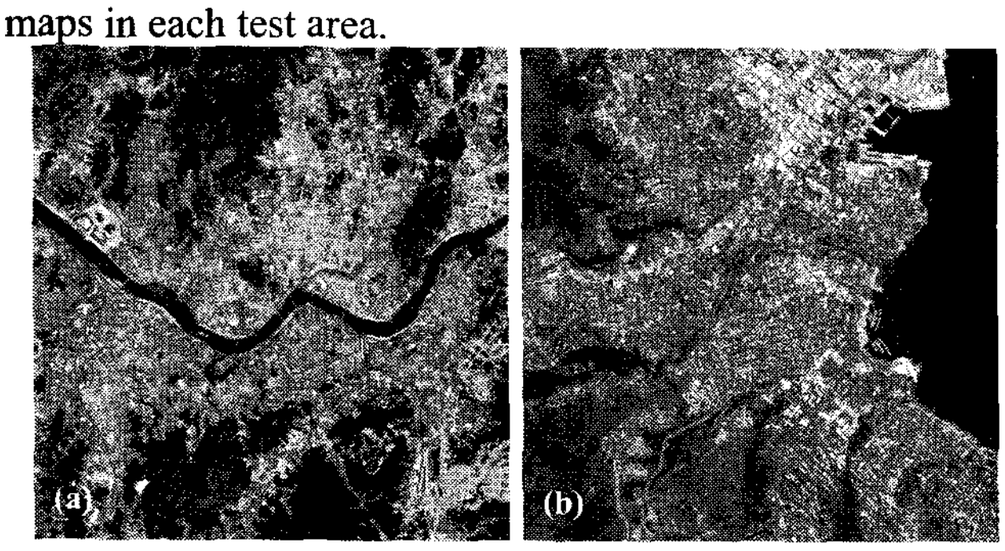

Figure 3. The test data: (a) Landsat7 ETM+ (30m) covered with Seoul, Korea; (b) Ikonos (4m) covered with Hobart, Australia.

The land cover map of figure 3(a) is provided by National Geography Information Clearinghouse of Korea (NGIC) and this map contains 6 classes: forest, water, grass, residential and commercial area, bare soil and field. The map can not be subdivided into individual building because of low resolution. The land cover map of Ikonos image is divided into residential area, forest, water, commercial area and grass (Figure 6(b)). The land cover map in test area is not offered officially so land cover map used this study is obtained from maximum likelihood classification with the 3D DWT coefficient. In previous study, the 3D DWT based classification method was more accurate than pixel based classification method in high resolution imagery. Therefore, we used 3D DWT based classification result for the land cover map of Ikonos image.

We input the number instead of class name in our discretion for the correlation analysis. More complex class is assigned to greater number. The correlation coefficients between UCI and land cover map are 0.41478 in Landsat7 ETM+ image and 0.42568 in Ikonos image. The positive correlation between UCI and class is shown weakly. Bare soil class make correlation coefficient low as this class has similar characteristics residential and commercial area class.

The variation on the UCI of each class using Landsat7 ETM+ image is displayed on figure 5(a). X-axis means UCI values and Y-axis represents the frequency of each class. The number of pixel is normalized by the total number of each class because the total number of class is different according to class. The variation of UCI can not be distinguished in figure 5(a), so the parts of figure 5(a) are enlarged (Figure 5(b)). Figure 5(b) shows the class frequency change according to UCI from zero to 1. Water class has the smallest energy parameter in all sub-bands because the reflectance of water is low in every band except blue band that is the first band. So, the UCIs of water class are concentrated in very low value. Forest class also have lower UCI. In case of grass and field classes, the peak of UCIs is seen earlier than bare soil and residential and commercial area. The UCI of residential and commercial area is the highest. However, as the color of bare soil is very bright like the color of residential and commercial area, it is difficult to distinguish residential or commercial area class from bare soil class.

The variation on the UCI of each class using Ikonos image is displayed on figure 7(a) and enlarged image is figure 7(b). Figure 7(b) shows the class frequency change according to UCI from zero to 3. The application case of Ikonos image is similar to Landsat image. Water class has the smallest UCIs. Forest and grass class also has very small UCI value. The UCIs are reached peaks in water, grass, forest, residential area and commercial area orders. Especially, commercial area shows very high UCIs. The correlation between UCI and class is higher at high resolution image. In high resolution image, residential and commercial area classes are distinct well as shown figure 7(b). The result of classification is represented as only class name. However, UCI can be expressed quantitative value. The greater UCI means more complex area. Therefore, this suggested index can be used for quantitative urban complexity estimation.

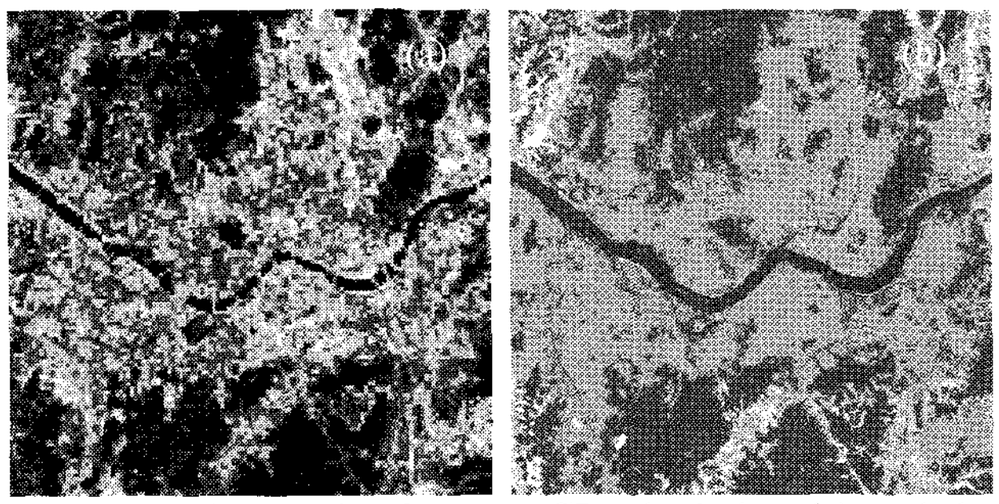

Figure 4. The result of 3DWUCI calculation (a) and the land cover map (b) in Seoul, Korea.

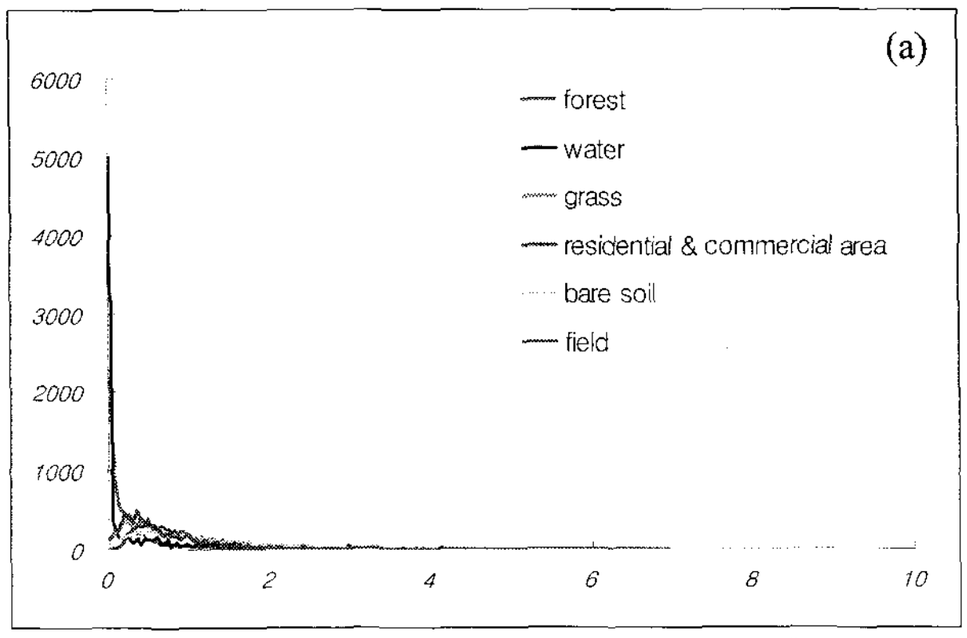

Figure 5. The histogram of 3DWUCI result using Landsat 7 ETM+ image (a) and the enlarged graphs (b).

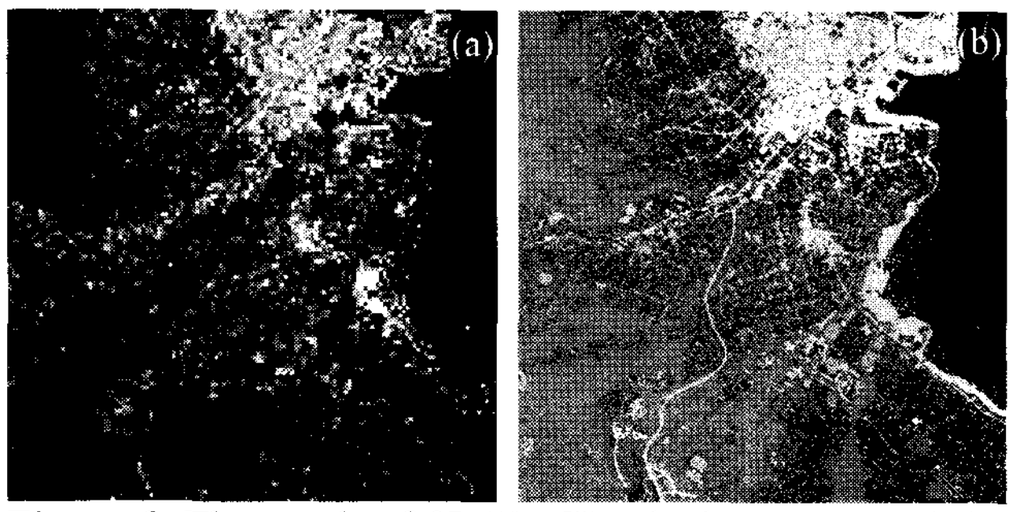

Figure 6. The result of 3DWUCI calculation (a) and the land cover map (b) in Hobart, Australia.

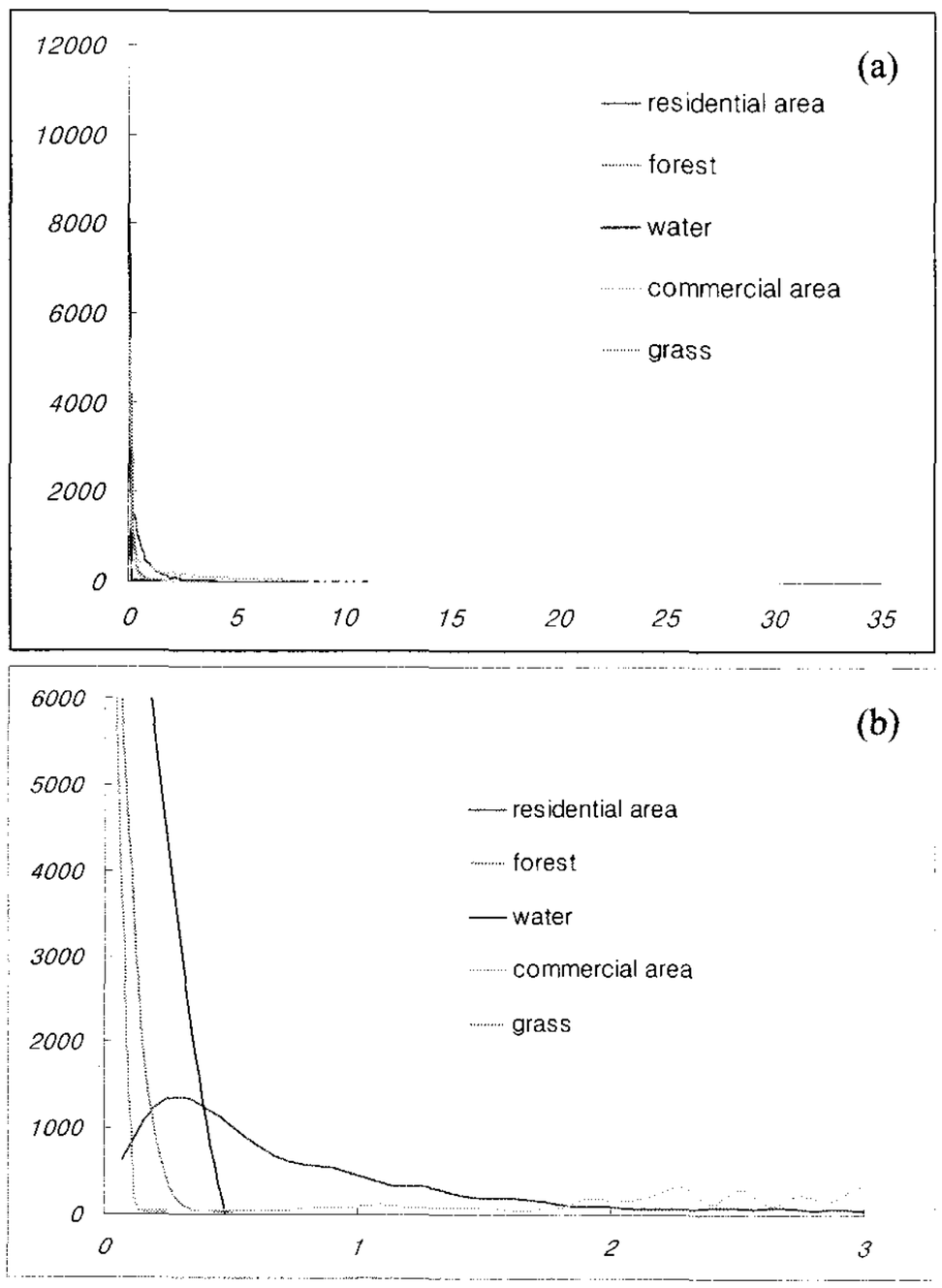

Figure 7. The histogram of 3DWUCI result using Ikonos image (a) and the enlarged graphs ((b).

5. CONCLUDING REMARKS

In this study, we propose the quantitative index to represent the standard of urban complex using the 3D wavelet transform and interpret with land cover map. Characteristics of each feature seen in urban image are analyzed using the difference between spatial variation and spectral variation through the energy parameter of the 3D DWT. Among the eight energy parameters of sub-bands, the ratio sum of H bands' energy parameters and sum of L bands' energy parameters in band direction is appropriate to present urban complexity. The suggested 3DWUCI could be used to express effectively the standard of urban complexity over a wide area using only satellite image not to use census. This index is expressed quantitative numerical value contrary to classification result. Therefore, it will be expected to use to the quantitative basic data analysis to grasp the relationship between urban and other components such as environment, weather, transportation and the quality of the life based on GIS (Geographic Information System) later on.

ACKNOWLEDGEMENTS

This work is financially supported by Korean Research Foundation (KRF) and Korean Aerospace Research Institutes (KARI). The part of the results in this study is granted by Korean Land Spatialization Group. The author (Yoo, H.Y.) is supported by the Brain Korea 21 project in 2007.

REFERENCES

Bederman, S. H., and Hartshorn, T. A., 1984. Quality of life in Georgia: the 1980 experience. *Southeastern Geography* **24**, pp. 78-98.

Chen, Z. and Ning, R., 2004. Breast volume denoising and noise characterization by 3D wavelet transform. *Computerized Medical Imaging and Graphics*, 28(5), pp. 235–246.

Forster, B., 1983. Some Urban Measurements from Landsat data. *Phorogrammetric Engineering and Remote Sensing*, 49(12), pp. 1693-1707.

Fukuda, S. and Hirosawa, H, 1999. A Wavelet-Based Texture Feature Set Applied to Classification of Multifrequency Polarimetric SAR Images. *IEEE Transactions on Geoscience and Remote Sensing*, 37(5), pp. 2282-2286.

Jun, B.W., 2006. Urban Quality of Life Assessment Using Satellite Image and Socioeconomic Data in GIS 2006. *Korean Journal of Remote Sensing*, 22(5), pp. 325-335.

Klock, H., Polzer, A. and Buhmann, J. M., 1997. Region-Based Motion Compensated 3D-Wavelet Transform Coding of Video. *In Proceedings of the 1997 IEEE International Conference on Image Processing*, pp..776-779.

Liu, B. C., 1976. Quality of Life Indicators in U.S. Metropolitan Areas, 1970. U.S. Environmental Protection Agency.

Lo, C. P. and Faber, B. J., 1997. Integration of Landsat Thematic Mapper and Census Data for Quality of Life Assessment. *Remote Sensing and Environment,* 62(2), pp. 143-157.

Weber, C. and Hirsch, J., 1992, Some urban measurements from SPOT data: urban life quality indices. *International Journal of Remote Sensing*, 13(17), pp. 3251-3261.

Yoo, H.Y., Lee, K. and Kwon, B.D., 2007, The Applicability of Spectral/Spatial Characterization and Classification using Multi-Spectral Satellite Imagery

based on 3D Wavelet Approach. *Proceedings of KSRS 2007 spring meeting* (In Korea)